Journal of Visualization, Vol. 2, Nos. 3/4 (2000) 301-308

Comparison of Techniques for Non-intrusive Fuel Drop Size Measurements in a Subscale Gas Turbine Combustor

Zaller, M.*[1], Locke, R. J.*[2] and Anderson, R. C.*[1]

*1 NASA Glenn Research Center, M.S. 77-1, 21000 Brookpark Road, Cleveland, OH 44135, USA.
*2 Dynacs Engineering Co., Inc., 2001 Aerospace Parkway, Brook Park, OH 44142, USA.

Received 28 June 1999.
Revised 30 September 1999.

***Abstract*:** In aviation gas turbine combustors, many factors, such as the degree and extent of fuel/air mixing, and fuel vaporization achieved prior to combustion, influence the formation of pollutants. To assist in analyzing the extent of fuel/air mixing, flow visualization techniques have been used to interrogate the fuel distributions during subcomponent tests of lean-burning fuel injectors. Combustor pressures (up to 14 bar) and air inlet temperatures (up to 680K) were typical of actual gas turbine engine operating conditions. Discrimination between liquid and vapor phases of the fuel was accomplished by comparing planar laser-induced fluorescence (PLIF) images, elastically-scattered light images, and phase/Doppler interferometer measurements. Estimates of Sauter mean diameters are made by ratioing PLIF and Mie scattered intensities for various sprays, and factors affecting the accuracy of these estimates are discussed. Mie calculations of absorption coefficients indicate that the droplet fluorescence intensities are proportional to their surface areas, instead of their volumes, due to the high absorbance of the liquid fuel for the selected excitation wavelengths.

***Keywords*:** combustor, fuel sprays, planar laser-induced fluorescence (PLIF), Mie scattering, drop size.

1. Introduction

To reduce the impact of aircraft engine emissions on the environment, and to meet proposed NO_x emission regulations, reduction of pollutant emissions from gas turbine combustors is required. For a given pressure and fuel/air ratio, pollutant production is influenced by the degree of fuel vaporization and mixing achieved prior to combustion. Due to the complexities of modeling and expense of conducting experiments on actual gas turbine combustors, some efforts have focussed on conducting tests at atmospheric pressure. Such tests have employed reacting and non-reacting fuel simulants, in attempts to recreate aspects of the actual two-phase flow, and to develop diagnostic techniques to measure parameters of interest.

Many researchers have characterized fuel concentrations, fuel/air ratios, and spray drop size distributions in swirl-stabilized spray flames and premixed, prevaporized subscale gas turbine combustors (e.g. Bulzan (1995), McDonell et al. (1995), Locke et al. (1998)). Phase Doppler interferometry (PDI) has been used to make spray drop size distribution and velocity measurements in spray flames, and to derive liquid mass flux from these parameters. Planar laser-induced fuel fluorescence has also been used to optically patternate sprays. Although PDI has become the standard technique for spray characterization, it is more difficult to align and time-consuming to apply than planar imaging, especially in high-pressure combustors with limited optical access.

Planar laser-induced fluorescence (PLIF) of fluorescein-doped methanol in a gas turbine swirl cup spray, at ambient pressure, was used to determine liquid phase fuel distributions (McDonell et al., 1995). Some agreement between fuel uniformity, as determined from images of the liquid fluorescence, and trends in NO_x emissions, was

obtained. Qualitative agreement between volume distribution measurements from PLIF and PDI was also demonstrated. From measurements of a monodisperse droplet stream, McDonell et al. (1995) determined that the relationship between droplet volume and PLIF image intensity was linear for their setup.

An innovative technique was developed (Herpfer and Jeng, 1995) to simultaneously measure the drop sizes and velocities in burning gas turbine injector sprays using planar imaging. They were able to achieve good agreement between PDI and their planar technique in reacting sprays; however, their setup had some difficulty with low signal-to-noise in regions of high flame luminosity. Their calculations show that the intensity of the Mie-scattered light is proportional to the square of the droplet diameter for their collection angle, droplet size parameter, and liquid optical properties.

PLIF imaging and planar Mie scattering have been combined (Yeh et al., 1995; Sankar et al., 1997), in non-vaporizing sprays, by ratioing PLIF and elastically-scattered light intensities, to determine spray volume-to-surface-area ratios. Since their sprays were not reacting, they ignored vaporized molecule fluorescence. Yeh et al. (1995) and Sankar et al. (1997) assumed that the accumulated PLIF image intensities were proportional to the summed droplet volumes, and the Mie signals, proportional to the sums of the drop cross-sectional areas. The ratios of the fluorescence and elastically-scattered light intensities for moderately absorbing droplets should equal:

$$\left(f \times \sum N_i d_i^3 + g \right) / \left(m \times \sum N_i d_i^2 \right) \tag{1}$$

where f and m are experimentally determined constants, g is the fluorescence arising from fluorophores in the gaseous phase, N is the number of drops in the ith size class, and d is the representative diameter of that size class. If g is negligible, then equation (1) is proportional to the Sauter mean diameter (SMD). We have applied this combination of fluorescence and elastically-scattered light to obtain planar measurements of liquid and gaseous fuel distributions in high pressure, reacting gas turbine combustor sprays.

2. Setup

Tests were conducted in the CE-5 Combustor Subcomponent Test Facility at the NASA Glenn Research Center for evaluation of low pollutant emission gas turbine injector concepts. Windowed combustor housings were used that allow optical access to reacting flows at pressures up to 2 MPa, and flow temperatures up to 2000K. Non-vitiated air is supplied to the test section at temperatures up to 840K. The fuel injector is positioned so that the dome face is visible within the 3.8 cm (axial dimension) view of the windows. Flow path dimensions for the housing used in this study were 7.6×7.6 cm. The inside surfaces of the windows, which are typically installed to be flush with the flow path formed by the ceramic liner, are cooled by a thin layer of gaseous nitrogen.

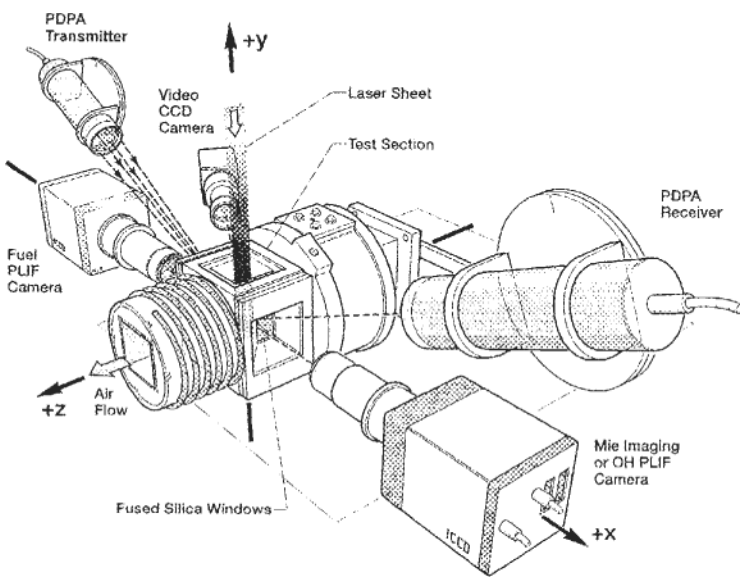

Fig. 1. Optical instrumentation layout around windowed gas turbine combustor.

The layout of the test section, along with laser-based instrumentation, is shown in Fig. 1. For the planar measurements, a Continuum Nd:YAG pumped dye laser with frequency doubling was used to generate approximately 18 mJ/pulse at 281.5 nm. The laser output, formed into a sheet using a 3000 mm focal length cylindrical lens, enters the top of the windowed test section. This 25 mm wide laser sheet is positioned to graze the injector exit, and is parallel to the y-z plane, with y defined as vertical, and z defined as the direction of the flow. To record images of fuel droplet scattering and fluorescence, a Princeton Instruments ICCD camera with a 384 × 576 element array was used. Two narrow band (10 nm FWHM) interference filters, one centered around 313 and another around 280 nm, enabled selective detection of fuel fluorescence and Mie scattering, as well as rejection of background combustor radiation. For these tests, the laser was tuned away from any OH absorption lines, so the 313 nm filter detected broadband fluorescence of the jet fuel, which arises primarily from polyaromatic hydrocarbons present in the fuel. Fluorescence spectra of room-temperature fuel samples have indicated that naphthalene-related compounds contribute to the UV fluorescence emission. An Aerometrics Phase/Doppler Particle Analyzer was also used to measure the size and velocity distributions of the fuel droplets for the relatively low air inlet temperature conditions presented here.

3. Results

The spray characteristics of two different types of injectors, with varying degrees of prevaporization, were analyzed in this study. The first flow field was produced by a lean burning, premixing, prevaporizing injector. At the idle operating condition (P=4 bar, T_{inlet}=620K), the combustor inlet temperature was too low to completely vaporize all of the fuel before injection into the combustor. Since the injection velocities were high to prevent flashback for this premixed configuration, the flame stabilized several inches downstream of the injector dome face.

A comparison between PDI temporal measurements of Sauter Mean Diameter (SMD), and concentration-sensitive drop size measurements derived from intensity ratios of the PLIF and Mie planar images, is shown in Fig. 2. Both data sets on the graph represent flow measurements acquired along a horizontal line, passing through the vertical center of the injector, and 6 mm downstream of the injector dome face. The images were binned by taking the averages of 4 × 4 blocks of pixels. Binning was necessary due to the unsteady nature of the flow, and also because the Mie and PLIF images were not acquired simultaneously. The trends between the PLIF/Mie ratios and the PDI drop size measurements are similar (Fig. 2). The most notable difference is the peak in the PLIF/Mie ratio at x=15 mm, which is not matched by the point SMD measurement. This degree of agreement is surprising, considering that the PLIF response is due to PAH in the vapor phase, as well as PAH in the liquid fuel droplets. It is postulated that the PLIF signals arising from the liquid and gaseous fluorescing phases happen to be similar, since higher vapor concentrations would be present in areas of higher liquid fuel drop number densities.

When cross-sections of the PLIF, Mie, and intensity ratios are compared (Fig. 3), the PLIF and Mie plots resemble each other closely, except that the PLIF peaks appear slightly broader, probably due to signals arising from vaporized PAH. Number densities of drops as measured using PDI are also presented (Fig. 3) for comparison with the Mie intensities. As would be expected, good agreement is seen between the plots of PDI number densities, and averaged Mie intensities, since both are related to the droplet concentrations.

Results from a second injector configuration, for which the fuel was not prevaporized, are presented in Fig. 4. This injector produced a hollow-cone spray at these operating conditions (P=14 bar), so PDI measurements were only obtained in fuel spray regions of higher number density, away from the injector centerline. Although PDI measurements were attempted across the entire diameter of the spray, the data rate was nearly zero for the negative x locations. This was attributed to multiple scattering effects induced by high number densities of very small droplets, which resulted in extinction of the scattered PDI signal. The agreement in this case between the imaging technique and PDI is not conclusive, but it could be argued that the relatively sparse PDI data are related to the PLIF/Mie ratio values.

As was the case with the prevaporized injector, good agreement is seen between the number density of drops as reported by the PDI, and the Mie intensities (Fig. 5). Since the trends in the PLIF and Mie plots are similar, when the PLIF is divided by the Mie signal, the highest ratio values occur just outside of the Mie peaks. This is somewhat disturbing, since it indicates that the highest PLIF/Mie values arise from vaporized fuel, instead of liquid droplets.

To illustrate this problem, slices of the PLIF and Mie signals, for different axial distances downstream of the injector, are shown in Fig. 6. Since the PLIF and Mie peak intensities are similar, when the image ratios are

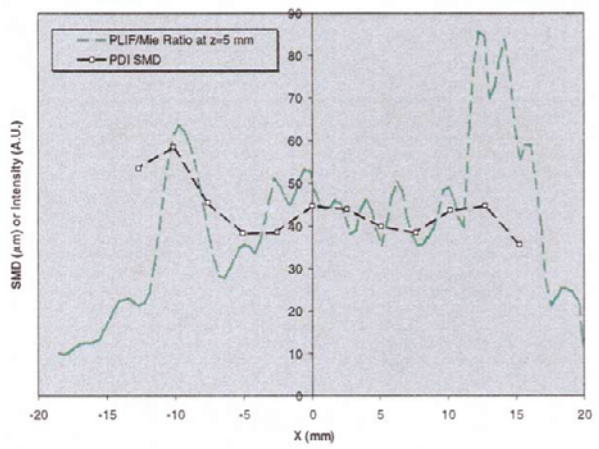

Fig. 2. SMD comparison of PDI and PLIF/Mie ratio for >95% prevaporized spray.

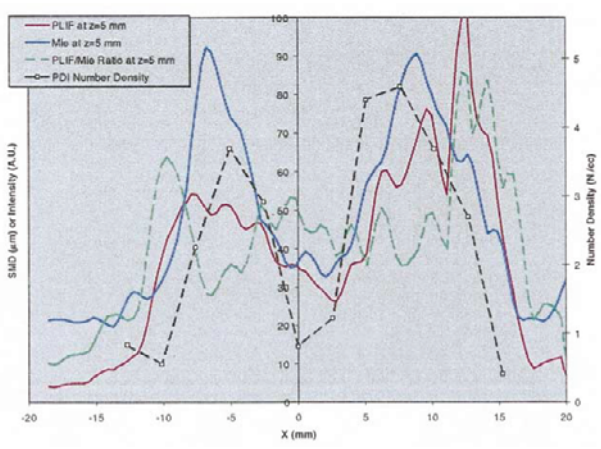

Fig. 3. PLIF, Mie, and PLIF/Mie ratios for prevaporized injector, with PDI number densities for comparison with scaled Mie.

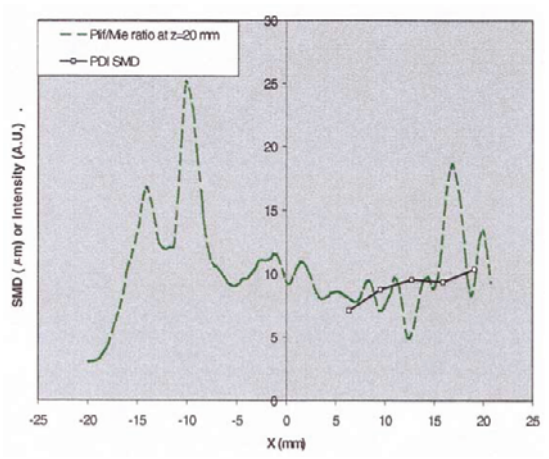

Fig. 4. SMD comparison of PDI and PLIF/Mie ratio for hollow cone spray.

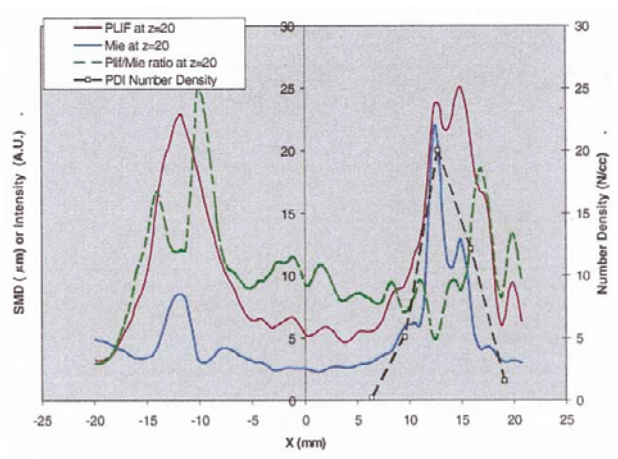

Fig. 5. PLIF, Mie, and PLIF/Mie ratios for hollow cone spray injector, with PDI number densities for comparison with scaled Mie.

taken, the peaks are replaced by gaps, generating an annular appearance for this hollow-cone spray. Although the PLIF and Mie images provide fantastic information about locations, relative concentrations, and extent of liquid and gas phase fuel distributions in these complex, high pressure, and high number density reacting spray flow fields, the image data are difficult to quantify. It appears that additional efforts will be required to resolve the difficulties introduced by PLIF detection of PAH in both liquid and gas phase.

To help resolve this difficulty with the fuel PLIF signals, the feasibility of using PLIF/Mie ratios to determine spray drop sizes for our setup was analyzed using a far-field Mie scattering code from Valley Scientific, Inc. The scattered light intensities were computed using a real refractive index, n, of 1.4, and a wide range of imaginary refractive indices, k. Other setup parameters included a detection angle of 90˚, and perpendicularly polarized incident light, with λ=.2815 μm. Computations were performed for drop diameters from 1 to 200 μm. Results are plotted in Fig. 7 as a function of x^2 (where $x=\pi d/\lambda$). For k larger than about .01, there is a linear relationship between the square of the droplet diameter and scattered intensity, even without performing any averaging over the receiving lens aperture. Absorbance data were used to calculate an imaginary refractive index of .045 at 281 nm for JP-5, indicating that the Mie signals were proportional to the squared droplet diameters for our experiment.

Absorption efficiencies, Q_{abs}, are plotted in Fig. 8 for the same parameters (n=1.4, λ=.2815 μm, 1<d<200 μm). If the fluorescence induced in the droplet is isotropic, then the absorption efficiency will indicate the

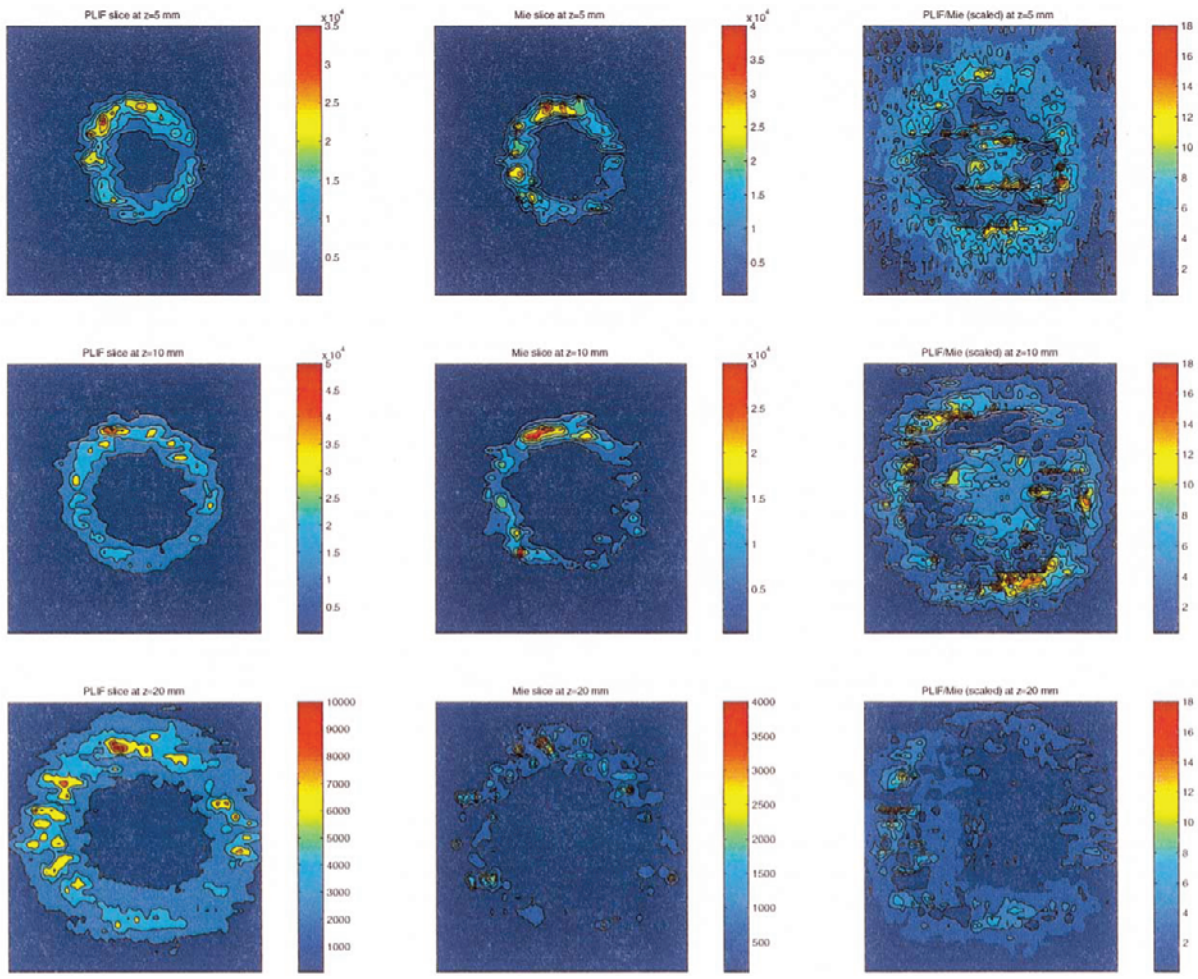

Fig. 6. Hollow cone spray PLIF, Mie, and ratio cross-sections 5, 10, and 20 mm downstream of the dome.

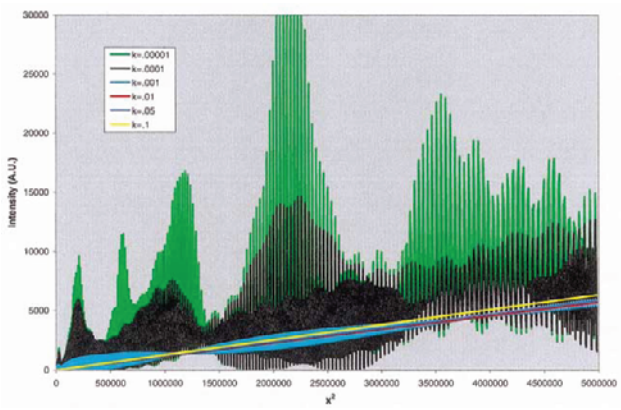

Fig. 7. Computed Mie-scattered intensities for various imaginary refractive indices. n =1.4, θ=90°, λ =.2815 μm.

relationship between droplet size parameter and fluorescence signal. Since Q_{abs} is normalized by the droplet cross-sectional area, $\pi d^2/4$, then a linear relationship between droplet size and Q_{abs} indicates that the drop fluorescence intensities are proportional to d^3. Unfortunately, it can be seen that only minimally absorbing drops exhibit absorption efficiencies that are linearly proportional to drop size (Fig. 8). For k greater than .0001, the relationship

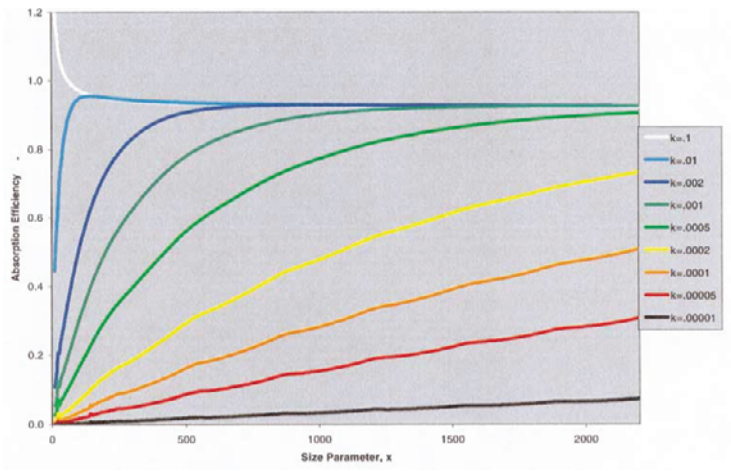

Fig. 8. Computed absorption efficiencies for various imaginary refractive indices. n=1.4, λ =.2815 μm.

between drop volume and fluorescence signal will not be linear for our droplet size range. In fact, for k>.01, the drop fluorescence intensity will be linearly proportional to the drop cross-sectional area, instead of its volume. This implies that for the PLIF/Mie ratioing technique to be successfully applied, the imaginary refractive index for the PLIF measurements should be .0001 or smaller. However, for fluorescence to occur, the liquid molecules must be absorbing, which implies larger k values. Since the imaginary refractive index of JP-5 is about .045 for the wavelength used in our tests, the PLIF signal responses were proportional to the squared droplet diameters, instead of the droplet volumes. This could explain why our PLIF and Mie signals nearly cancelled each other out. If our PLIF and Mie signals were both proportional to the drop cross-sectional areas, then their ratios should have been a constant: if not for the vapor fuel response of the PLIF, our signal ratios would have been nothing but noise.

A linear relationship was claimed (Rotunno et al., 1990) between droplet volume and fluorescence intensities for droplets with an optical density of 0.2 or less. They considered a maximum drop size parameter of 530 for their exciplex fluorescence experiment. An optical density of 0.2 corresponds to an imaginary refractive index of .0002 at their wavelength of 355 nm. This agrees with the computations presented in Fig. 8, since the k=.0002 line is fairly straight for size parameters from 10 to 530, whereas curvature is visible in the slightly more absorbing k=.0005 data over the same size range.

The differences in the internal intensities for minimally and highly absorbing drops were computed using Mie scattering code for spheres (Barber and Hill, 1990). Although these internal intensities are for the incident wavelength only, it is assumed that the fluorescence signal will be proportional to the intensity of the exciting laser light. Cross-sections of the logarithm of the Mie intensities are plotted in Figs. 9 and 10 for size parameters of x=10 and x=100. The incident linearly polarized wave propagates from the bottom to the top in these figures. Figure 9 shows the cross-section intensities for all intensity values within the drop radii. The same data are plotted in Figure 10, except that the ranges of contour values were limited to 4 orders of magnitude. A low k value of .0001 was used in the computations on the left side, and our estimated k value (.045 for JP-5 at 281 nm) in the plots on the right. For very tiny drops (x=10), the Mie intensities are similar for both k values (Figs. 9a and 9b). Light passing through the droplet is internally reflected multiple times to produce an interference pattern, with a focus opposite the incident beam. However, if the drop sizes are increased to x=100, it can be seen that the highly absorbing drop (Fig. 9d) has most of the intensity absorbed near the droplet surface. In the less absorbing case (Fig. 9c), the interfering internally reflected light, as well as the focus at the top of the plot, can be seen.

When the same results are plotted, except using contour values that are limited to four orders of magnitude, the similarities between the x=10 droplets for k=.0001 and k=.045 are still apparent (Figs. 10a and 10b). However, for a size parameter of x=100, the difference between intensity fields for the low and high imaginary refractive indices is emphasized (Figs. 10c and 10d). Despite the relatively small drop diameter of d=9 microns, all of the light incident on the k=.045 drop is absorbed near the surface, without passing through the drop to form any interference pattern, or foci. This explains why the highly absorbing drops (k=.045) would have a fluorescence signal proportional to their surface areas, instead of their volumes.

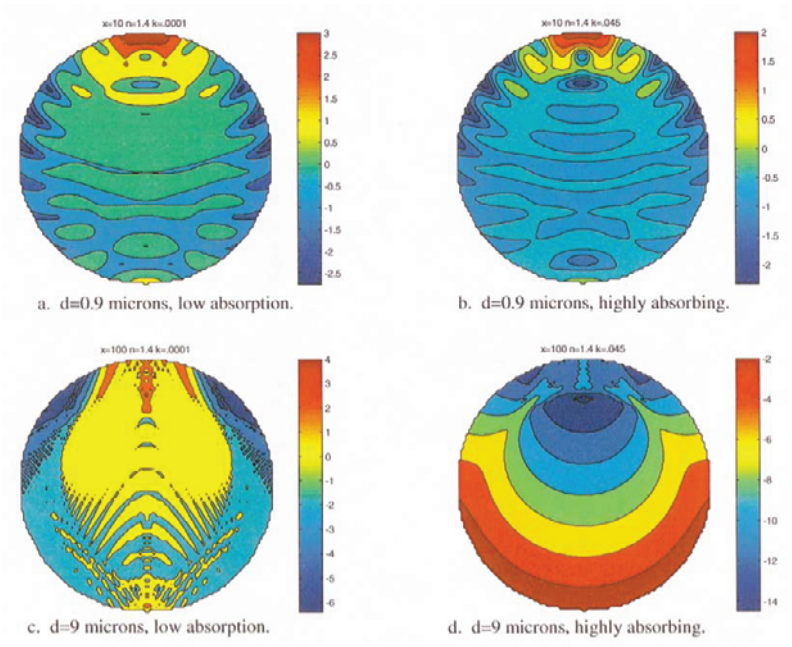

Fig. 9. Logarithm of computed cross-section Mie intensities, for two droplet sizes and absorbances.

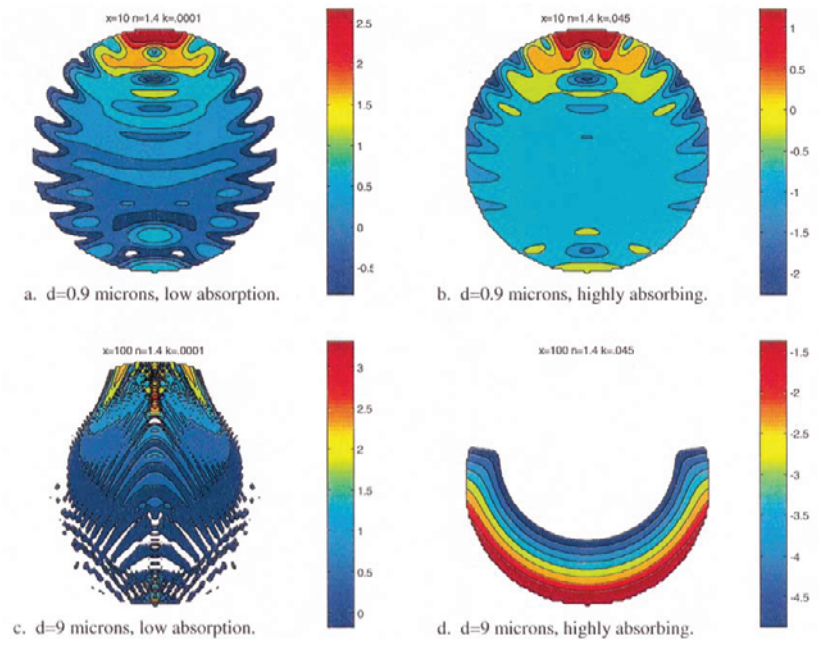

Fig. 10. Logarithm of computed cross-section Mie intensities, for two droplet sizes and absorbances, with limited contour intensity ranges.

4. Conclusions

Comparisons between PDI measurements and PLIF/Mie images were conducted on high pressure gas turbine combustor flow fields. Although some similarities between the drop sizes were apparent for tests on a prevaporizing injector, conclusive agreement between PLIF/Mie and PDI Sauter mean diameters was not demonstrated on a hollow cone spray with direct fuel injection. It appears that the Mie and PLIF signals were related to the drop number densities, which makes the combination of these techniques invaluable for rapid determination of liquid and vaporized fuel distribution over large regions of the combustor.

Mie scattering calculations indicate that although the elastically-scattered light intensities are proportional to the drop cross-sectional areas, the PLIF response for our laser wavelength and fuel imaginary refractive index did not produce a signal that is proportional to the droplet volumes. Additional work is required to determine the error introduced by the PLIF response to gaseous and liquid phase fuel, since the liquid phase response may not be linear, or may even be non-existent, and the gas phase measurements need to be accounted for before the PLIF/Mie ratio is computed. Although these analyses are preliminary, they have been invaluable in determining the sensitivity of the derived values to such factors as laser wavelength, laser power fluctuations, flow field oscillations, and beam polarization direction. Future work will include attempts to elicit droplet fluorescence at wavelengths for which the fuel is less absorbing, which would make the fluorescence signal proportional to the droplet volumes. We also expect to study the differences in extent and response of the fluorescence signals arising from both gas and liquid phase fuel, as well as Mie-scattered intensities, to obtain information about fuel/air mixing, and the relationship between fuel/air uniformity and combustor emissions.

References

Barber, P. W. and Hill, S. C., Light Scattering by Particles: Computational Methods, (1990), World Scientific Publishing Co., Singapore.

Bulzan, D. L., Structure of a Swirl-Stabilized Combusting Spray, J. Prop. Power, 11-6 (1995), 1093-1102.

Herpfer, D. C. and Jeng, S. M., Streaked Particle Image Velocimetry and Sizing in Burning and Non-Burning Sprays, 33rd Aerospace Sciences Meeting and Exhibit (Reno), (1995), AIAA Paper No. 95-0141.

Locke, R. J., Hicks, Y. R., Anderson, R. C. and Zaller, M. M., Optical Fuel Injector Patternation Measurements in Advanced Liquid-Fueled, High Pressure, Gas Turbine Combustors, Combust. Sci. Tech., 138 (1998), 297-311.

McDonell, V., Lee, S. and Samuelsen, S., Interpretation of Spray Behavior in Complex Aerodynamic Flows Using Phase Doppler Interferometry and Planar Liquid Laser Induced Fluorescence, Proc. SPIE, Optical Techniques in Fluid, Thermal, and Combustion Flow, 2546 (1995), 530-539.

Rotunno, A. A., Winter, M., Dobbs, G. M. and Melton, L. A., Direct Calibration Procedures for Exciplex-Based Vapor/Liquid Visualization of Fuel Sprays, Combust. Sci. and Tech., 71 (1990), 247-261.

Sankar, S. V., Maher, K. E., Robart, D. M. and Bachalo, W. D., Rapid Characterization of Fuel Atomizers Using an Optical Patternator. Proceedings of ASME Asia '97 (Singapore), (1997).

Yeh, C. N., Kosaka, H. and Kamimoto, T., Measurement of Drop Sizes in Unsteady Dense Sprays, in *Recent Advances in Spray Combustion: Spray Atomization and Drop Burning Phenomena*, (1995), AIAA, Reston, VA, 297-308.

Author Profile

Michelle Zaller: She received her B.S. and M.S. in Mechanical Engineering from Case Western Reserve University in Cleveland Ohio. She has been conducting combustion research at the NASA Lewis (now Glenn) Research Center since 1988, performing experimental investigations on optically-accessible rocket engines, as well as on numerous liquid-fueled air-breathing engine combustor configurations. Her primary interest has been application of optical diagnostics to subscale combustors, with special focus on studying the impact of critical phase transition effects on propellant mixing in high pressure propulsion systems.

Randy J. Locke: He earned his Ph.D. in Physical Chemistry at Wayne State University in Detroit Michigan where he studied intramolecular/intermolecular photoassociation processes. He was a National Academy of Science/National Research Council (NAS/NRC) Postdoctoral Associate, at the U. S. Army Research Laboratory (ARL), Aberdeen Proving Ground, MD. While at the ARL he performed optical studies on low pressure gaseous flames, laser-induced microplasma formation, and laser-induced ignition of solid propellants. For the past 9 years he has studied high pressure combustion processes for aerospace propulsion applications. His main research interests are to gain a detailed understanding of the physical processes inherent in reacting, high pressure flows via advanced laser diagnostic techniques. He is the author of 12 open literature papers and 30 technical reports and government publications.

Robert C. Anderson: He received his Bachelor of Engineering Science (Physics) degree at Cleveland State University in 1966 and his Masters in Engineering Science from the University of Toledo in 1971. He has worked on the development of advanced instrumentation systems throughout his career at the NASA Glenn Research Center, in Cleveland Ohio. Technical areas of interest have included dynamic pressure measurement, smoke measurement, gas analyzer systems, and currently advanced laser diagnostics for combustion research.